Synthetic Metals 268 (2020) 116483

Contents lists available at ScienceDirect

Synthetic Metals

journal homepage: www.elsevier.com/locate/synmet

Self-discharge characteristics of vapor deposited polymer electrodes in an all-textile supercapacitor

Wesley Viola[a], Chang Jin[b], Trisha L. Andrew[a,c,*]

[a] Department of Chemical Engineering, University of Massachusetts Amherst, Amherst, MA USA
[b] Amherst Regional High School, Amherst MA USA
[c] Department of Chemistry, University of Massachusetts Amherst, Amherst, MA USA

ARTICLE INFO

Keywords:
Wearable supercapacitor
Self-discharge
Charge redistribution
PEDOT
Polymer energy storage
Oxidative chemical vapor deposition

ABSTRACT

Despite the many efforts put toward developing flexible supercapacitors for wearable technology, few studies have focused on self-discharge, the spontaneous voltage decay of devices stored in their charged state. In this work, we characterize the self-discharge behavior of an all-textile supercapacitor utilizing oxidative chemical vapor deposited (oCVD) PEDOT-Cl electrodes. A significant portion of the voltage losses are found to arise from charge redistribution, a physical process involving the rearrangement of charges within the electrode material. Two means of mitigating this mode of self-discharge are presented. A post-charging hold step improves voltage retention by enabling spatially-uniform charge distribution within the electrode. Improving the ordering of polymer crystal domains via control over the polymer growth temperature during oCVD is also found to impact the self-discharge rate. Electrochemical and morphological characterizations of films grown at high and low temperature indicate that more ordered polymer films exhibit less self-discharge due to charge redistribution, perhaps a result of greater charge accessibility throughout the film. These results, including improved charging protocols and material optimizations, may help pave the way for practical, lightweight charge storage devices to power wearable electronics.

1. Introduction

Improved wearable energy storage is a major barrier to developing many emerging on-body health monitoring and consumer technologies. In such applications, device performance metrics matter only insofar as how the end-user experiences the physical form factor, flexibility and aesthetics of a wearable device. The development of flexible and lightweight electrodes on suitable substrates is key to realizing widespread adoption of next-generation electronics.

Conjugated polymers are a competitive material choice, possessing the appropriate flexibility, processability, and charge capacity for wearable energy storage devices. Being soft materials, conjugated polymers have the necessary mechanical properties to flex and deform, readily adapting to body movements, as well as resisting delamination on flexible substrates. While possessing desirable mechanical properties, conjugated polymers are also amenable to a variety of processing techniques including screen printing, inkjet printing, and vapor deposition [1–3]. Vapor deposition of conjugated polymers specifically achieves robust, conformal coatings on ordinary textiles for seamless integration of wearable devices with ordinary garments. With both good device metrics and the unmatched pliability and feel of natural fabrics, such wearable devices have the potential for widespread adoption [2].

Flexible energy storage has recently attracted much interest. While advances have been made to improve key device metrics such as energy density, power density, cycle stability, and safety, efforts into studying the self-discharge of electrochemical capacitors have been scarce [4]. Self-discharge is the spontaneous voltage decay of charged capacitors stored at open circuit. Despite the power and cycle stability advantages of supercapacitors, self-discharge rates are often higher compared to batteries [5,6]. The practical importance of self-discharge in energy storage is obvious, and translation of new polymer supercapacitor technologies into functional circuits requires an understanding of this process and its mechanisms.

Charging a supercapacitor involves bringing the electrodes to a high energy state. If a pathway exists to lower the energy of the system, self-discharge will spontaneously occur. Three modes of self-discharge have been identified: ohmic leakage, [5,7,8] parasitic redox reactions [5,7,8], and charge redistribution [9–11]. Ohmic losses are simply due to an electronic short between the electrodes, i.e. when a separator fails

* Corresponding author at: Department of Chemical Engineering, University of Massachusetts Amherst, Amherst, MA USA.
E-mail address: tandrew@umass.edu (T.L. Andrew).

https://doi.org/10.1016/j.synthmet.2020.116483
Received 16 April 2020; Received in revised form 16 June 2020; Accepted 20 June 2020

to prevent electrode-electrode contact. Parasitic redox reactions involve a charge transfer from the electrodes to impurities or redox-active species in the system. An example of such impurities are transition metal ions that may act as redox-shuttles, dissipating charge between the anode and cathode [12,13]. The associated time dependence of voltage decay can offer insight into the specific self-discharge mechanism: diffusion limited discharge is square-root dependent on time, whereas activation controlled discharge is log-dependent [14,15]. Charge redistribution is a distinctly physical process that arises when, during charging, ions accumulate at high-low resistance interfaces, for example at the mouths of micropores in activated carbon, and subsequently redistribute throughout the material. A higher density of charge yields a higher electrode surface potential that diminishes as the charges diffuse through higher resistance regions.

In this work, we study the self-discharge behavior of a high-loading, all-textile charge storage device comprised of two conducting polymer-coated fabrics as the active electrodes. The enabling pseudocapacitive polymer coating on these fabric electrodes is a persistently *p*-doped conducting polymer, poly(3,4-ethylenedioxythiophene)-chloride (PEDOT-Cl), that we vapor deposit onto carbon cloth using a custom-built hot wall reactor. We have previously reported on and extensively characterized textile energy storage devices utilizing this material which achieved areal capacitances of 80 m F/cm^2 [2,16]. Similar to other pseudocapacitive inorganic materials (transition metal oxides like RuO_2), we find that the self-discharge in vapor-deposited PEDOT-Cl is in large part due to charge redistribution. Among the scarce studies on self-discharge of conducting polymer electrodes, [12–19] none to our knowledge have identified charge redistribution as a mechanism for self-discharge. Two means of mitigating this particular type of self-discharge are proposed. A pre-conditioning “hold step” uniformly diffuses charges throughout the electrode and improves device voltage retention. Further, material properties of the polymer electrodes may be optimized by control over the polymer growth temperature. We observe a correlated impact on self-discharge rates, with higher temperature film growth leading to reduced self-discharge. It has been previously shown that vapor deposited PEDOT-Cl transitions from more polycrystalline to more ordered with increasing growth temperature. Drawing on work that identified charge redistribution in pseudocapacitive RuO_2 as originating from high accessibility “outer regions” and low accessibility “inner regions”, we propose that the polycrystalline films grown at low temperatures have a greater fraction of inaccessible sites into which charge is leaked (redistributed) over long times (hours), contributing to self-discharge. Control over the polymer morphology offers another means of mitigating self-discharge in these polymer textile electrodes.

2. Results and discussion

2.1. PEDOT-Cl deposition and substrate temperature-dependent film properties

Thick films (~1 μm) of persistently *p*-doped PEDOT-Cl were vapor deposited in a custom-built chamber depicted in Fig. 1a. Control of the substrate stage temperature (i.e. the temperature at which the polymer grows) in oxidative chemical vapor deposition (oCVD) processes can greatly affect the morphological and electronic properties of the resulting polymer films [20,21]. Here, PEDOT-Cl was grown at high (150 °C) and low (50 °C) substrate temperatures (T_{stage}).

To investigate differences in the two materials, we characterized their electronic and electrochemical properties. Films on glass deposited at high temperatures had higher conductivities measured with a four-point probe (317 ± 19.5 mS/cm versus 98.5 ± 2.5 mS/cm, respectively). Three electrode, volumetric cyclic voltammetry (CV) scans of these films are shown in Fig. 1c. The significantly larger currents maintained by the 150 °C films indicate a higher specific capacitance relative to 50 °C films, suggesting greater electrochemical accessibility throughout the film. Gravimetric capacitances are found to be 149 F/g and 106 F/g for 150 °C and 50 °C films respectively. Assuming a density of 1.3 g/cm^3 [20], the doping fraction (fraction of doped EDOT units), is 22 % and 16 % for 150 °C and 50 °C films respectively.

Having characterized the growth temperature-dependent properties of PEDOT-Cl, we next sought to investigate how these materials performed in an all-textile supercapacitor, with a specific focus on their self-discharge behavior.

2.2. Device structure and characterization

The textile supercapacitors were comprised of symmetric PEDOT-Cl-coated carbon cloth electrodes. The electrodes, spaced apart by two uncoated cotton separators, were stacked and saturated with a non-acidic gel electrolyte (PVA/LiCl) to make a flexible, symmetric device (Fig. 2a). Galvanostatic charge-discharge (GCD) curves over a range of current densities showed triangular profiles, indicating highly reversible energy storage (Fig. 2a). Comparable two electrode cyclic voltammetry scans also demonstrate square-shaped capacitive charging (Fig. 2c). More than 90 % of the initial capacity was maintained over 20,000 GCD cycles (Fig. 2b). This remarkable cycle stability is not common among conjugated polymers and is owed to the unique chemical stability of PEDOT-Cl which has been characterized in prior reports [16,22,23]. However, despite demonstrating high cycle stability, PEDOT-Cl electrodes also exhibit high self-discharge rates: upon charging and switching to open circuit, 50 % of the initial stored charge is lost after five hours. In this work, we sought to understand and improve this electrode property that is often overlooked in the emerging polymer supercapacitor community.

2.3. Self-discharge by parasitic redox reactions

As discussed above, redox-active contaminants in the electrochemical cell may contribute to self-discharge, so we first considered two potential contaminants in our system: iron oxidant residues from the vapor polymerization process and oxygen from ambient air.

To investigate the role of iron, three PEDOT-Cl electrodes with varying amounts of residual oxidant contamination were intentionally created by varying post-deposition rinse times, where shorter times left behind higher concentrations of iron salt residues (a mixture of Fe^{2+} and Fe^{3+} chloride and/or sulfate salts). These three samples showed no significant differences in self-discharge behavior (Figure S1a). The sample subjected to the longest rinse time (72 h) was analyzed using inductively coupled plasma mass spectrometry (ICP-MS), which showed residual iron (and other transition metal) concentrations in the parts per billion range (Fig. 3a). Based on prior studies of iron contamination in carbon-based electrodes, this concentration was too low to make an impact on self-discharge [13].

The role of oxygen contamination was evaluated by measuring self-discharge of devices in ambient air and in a nitrogen flushed glovebox. Devices operated in ambient showed worse voltage retention, presumably due to the reduction of ambient oxygen at the cathode (Fig. 3b) [24]. An air-impermeable packaging material may be necessary to limit this mode of self-discharge.

2.4. Charge redistribution of devices and impact of polymer growth temperature

One mode of self-discharge identified for electric double layer capacitors (EDLCs) and transition metal oxide pseudocapacitors is charge redistribution, or the reorganization (equilibration) of charges between physical regions of high and low accessibility in the electrode material [4,9,25]. Suspecting a parallel with our PEDOT-Cl supercapacitors, which store charge in a similar manner, we incorporated a “hold step,” where the device was subjected to a constant applied potential of 800 mV following charging at 5 mV/s to allow for full charge saturation

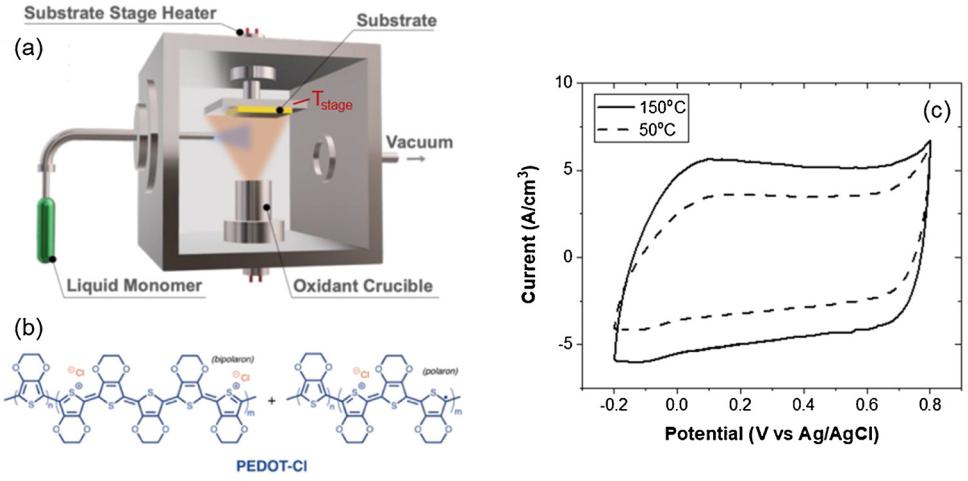

Fig. 1. PEDOT-Cl deposition and film electrochemistry dependence on polymer growth temperature (T_{stage}). (a) Vacuum chamber used to carry out oxidative chemical vapor deposition (oCVD) of PEDOT-Cl on textiles. (b) Oxidized, charge-carrying units of PEDOT-Cl. (c) Three-electrode cyclic voltammetry of films deposited at T_{stage} = 150 °C and 50 °C on glass.

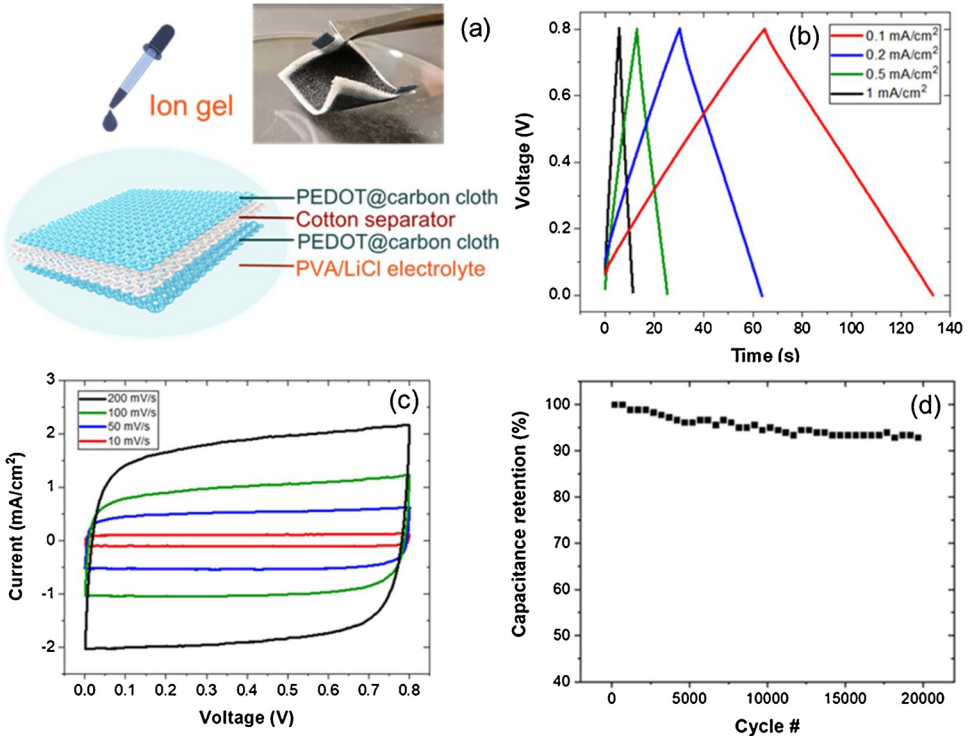

Fig. 2. Supercapacitor structure and characterization of device using PEDOT-Cl electrodes grown at T_{stage} = 150 °C. (a) Flexible, all-textile supercapacitor with symmetric PEDOT-Cl coated cotton electrodes and a polymer electrolyte. (inset) Photograph of assembled device. (b) Galvanostatic charge-discharge (GCD) curves over a range of currents normalized to device area. (c) Two electrode cyclic voltammetry. (d) Capacitance retention across 20,000 cycles of GCD performed at 2 mA/cm^2.

(a)

Analyte	Concentration (ppb)
Fe	39.687
Zn	5.986
Ni	3.578
Cu	2.654
Cr	1.244
Ag	0.581
Mn	0.273
Pb	0.185
Zr	0.106
Sc	0.1
Mo	0.092

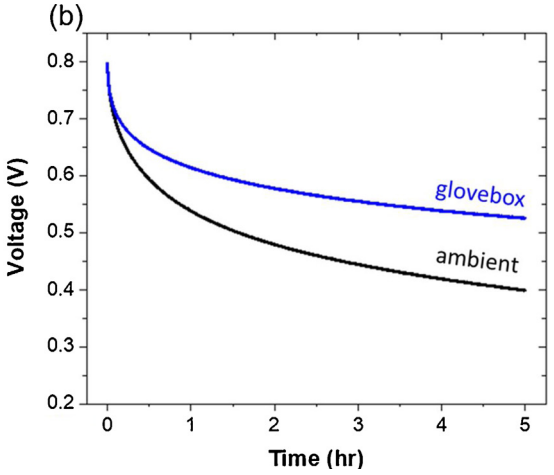

Fig. 3. Influence of contaminants and ambient operating environment on self-discharge in the PEDOT-Cl system. (a) ICP-MS of PEDOT-Cl electrodes following a 72-h solvent soak to remove metal salts. (b) Self-discharge characteristics of devices in glovebox (blue) and ambient (black). (For interpretation of the references to colour in this figure legend, the reader is referred to the web version of this article). The PEDOT-Cl layer was grown at T_{stage} = 150 °C.

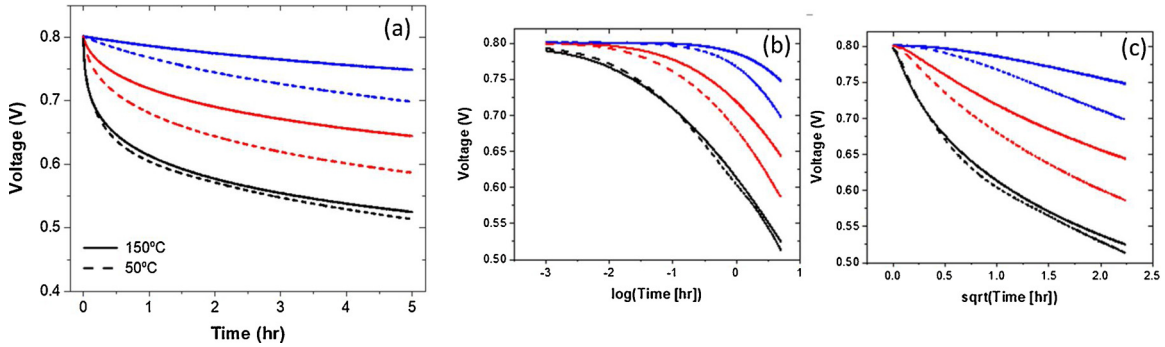

Fig. 4. Self-discharge characteristics of textile devices with PEDOT-Cl layer grown at T_{stage} = 150 °C and 50 °C. (a) Open-circuit voltage decays of devices with varying post charge hold steps - no hold (black), 1-minute hold (red), and 3 -h hold (blue). Replots in (b) log[time] and (c) sqrt[time]. (For interpretation of the references to colour in this figure legend, the reader is referred to the web version of this article).

of the electrodes. Fig. 4a shows typical self-discharge decays at open circuit with no hold step (black), after holding for one minute (red), and after holding for three hours (blue). The self-discharge behavior of devices constructed using PEDOT-Cl films grown at a high and low temperature were also compared. For both devices, self-discharge rates diminish with longer hold times, suggesting that charge redistribution plays a role. Also, after the first cycle, 150 °C devices show significantly better voltage retention than 50 °C devices after both one-minute and three-hour hold steps.

To understand this behavior further, we replotted the self-discharge data in log time (Fig. 4b) and square-root time (Fig. 4c), as has been previously shown to give insight into the decay mechanism [4]. For faradaic, activation-controlled processes, voltage decays are linear in log time, while diffusion-controlled processes are linear in square-root time. Both devices display the same qualitative trend. Initially the behavior is more characteristic of a faradaic, activation-controlled process (log dependence). This may be due to an initial irreversible oxidation of polymer segments, as has been previously reported for cycled PEDOT-Cl [20]. CV scans before and after self-discharge cycling also show a profile change consistent with such an oxidation at higher potentials, with 50 °C devices showing a more dramatic change (Figure S2).

At longer hold times, the voltage decay becomes linear in square-root time, indicating a transition to self-discharge dominated by a diffusion-controlled process. This behavior may be akin to the diffusion-controlled charge redistribution previously identified for transition metal oxide pseudocapacitors like RuO_2. In such materials, there exist "outer" regions that charge quickly and, upon switching to open circuit, dissipate into slower responding "inner" regions by a transport process linear in square-root time [9,25,26]. The reverse is also expected when the film is equilibrated in a charged state and then discharged—outer regions should discharge quickly and, upon switching to open circuit, inner regions should slowly feed charges to the outer regions, causing a voltage rebound. Indeed, we observed this phenomenon for our PEDOT-Cl electrodes (Fig. 5a), with the 50 °C film showing a more severe voltage rebound (i.e. more severe charge redistribution). These observations lead us to conclude that, in both cases, a hold step acts to fully equilibrate both the outer and inner regions of the PEDOT-Cl electrode, improving voltage retention (Fig. 5b).

Observing significant differences in the self-discharge rate between polymer electrodes grown at high and low temperature, one might expect to see a corresponding difference between impedance spectra, specifically the Warburg element, if the self-discharge is governed by a diffusion-limited process. Electrochemical impedance spectroscopy (EIS) of the two all-textile devices, fitted with a Randles circuit, indeed show this (Fig. 6a). Devices made with polymer electrodes grown at 50 °C exhibit significantly higher Warburg and charge transfer resistances (11.5 ± 1.5 Ω and 1.0 ± 0.04 Ω, respectively) relative to electrodes grown at 150 °C (7.6 ± 0.3 Ω and 0.29 ± 0.02 Ω, respectively). Given that the Warburg element arises from diffusion-controlled charge transport (that should follow a square-root time dependence) [27], this result is consistent with the higher rate of diffusion-controlled self-discharge observed for low temperature devices.

With this picture of charge redistribution, the higher self-discharge rate of the 50 °C device can be understood in the context of growth temperature-dependent film properties. We believe that the key difference between the high and low temperature films is crystal morphology – this difference has been dissected in recent reports [20,21,28]. Our own X-ray diffraction characterizations (Fig. 6b) of the high and low temperature films are consistent with these prior reports. For high temperature films, a sharp, high intensity peak is observed at 2Θ = 6.5°, corresponding to an edge-on crystallite orientation with long-range order. Low temperature films exhibit a very weak peak at 6.5°; no other strong features are seen, suggesting a mixture of randomly-oriented (isotropic) crystallites.

The lower specific capacitance seen earlier for the 50 °C film suggests hindered ion accessibility, consistent with the self-discharge and impedance results. This correlation implies that more ordered morphologies in PEDOT-Cl result in improved ion transport behavior. At first, this seems to conflict with a recent report of another conjugated polymer, poly(3-hexylthiophene) (P3HT), exhibiting inhibited ion uptake in crystalline regions versus amorphous regions [29]. Based on XRD (absence of broad features) and DSC (Figure S3) characterizations of high and low temperature PEDOT-Cl films, we conclude that there is no significant amorphous fraction in either sample (i.e. the degree of crystallinity is the same in both samples). In this case, the entire volume of the films is paracrystalline and disorder arises as randomized (isotropic) crystallite orientation. Other reports on vapor deposited and electrochemically polymerized PEDOT-Cl have also shown an absence of amorphous character in films, distinguishing these forms of PEDOT-Cl from other solution-processed conjugated polymers/composites, such as P3HT and PEDOT:PSS [20,21,28,30]. Given the existence of ordered dopant ion planes within a PEDOT-Cl crystal [31], it is reasonable to expect more torturous (hindered) ion transport in more disordered, polycrystalline films. Such morphology-dependent ion dynamics may explain the improved electrochemical performance of high temperature grown PEDOT-Cl films observed here and highlights differences from other conjugated polymers.

3. Conclusion

Here we investigate the self-discharge behavior of a pseudocapacitive material, PEDOT-Cl, as it is applied to an all-textile charge storage device. We show that charge redistribution, a physical reorganization of ions within the film, accounts for a significant amount of the observed voltage losses. Variation in the self-discharge behavior was observed for polymer electrodes vapor deposited at high and low temperatures. Characterizations of the two polymer samples indicate a more disordered crystal structure for the low temperature films with

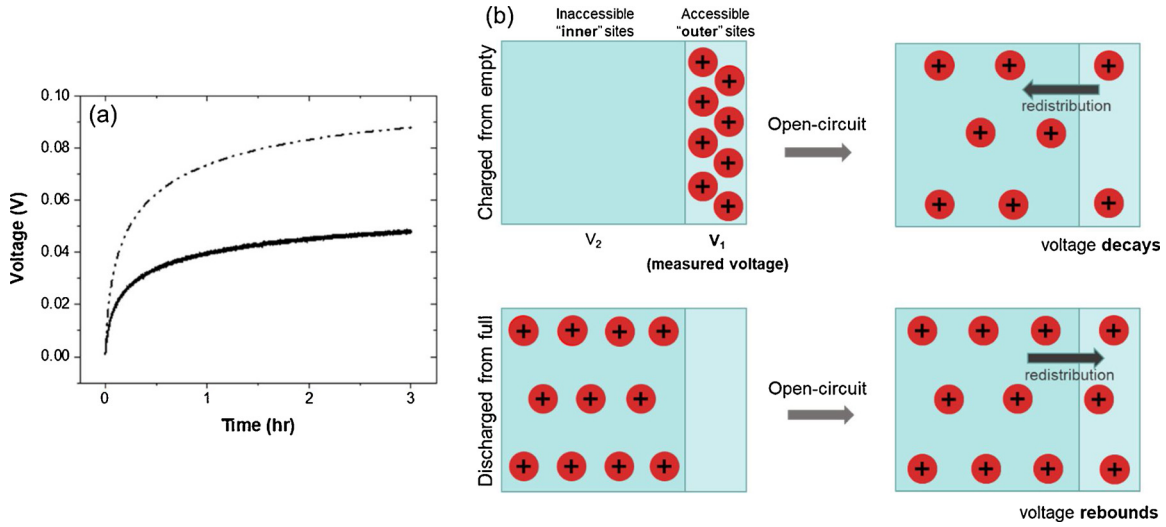

Fig. 5. Voltage rebound and charge redistribution. (a) Voltage rebound curves of 150 °C (solid) and 50 °C (dashed) devices. (b) Illustration of charge redistribution following charging and discharging.

correspondingly lower doping fractions and limited charge transport characteristics. We propose that self-discharge due to charge redistribution is exacerbated in these samples due to the existence of regions of low charge accessibility, possibly at the misoriented crystal boundaries. Variation in the polymer growth temperature affords control over this self-discharge property.

As a matter of practical importance for integrating flexible energy storage devices into functional systems, self-discharge of conjugated polymer-based electrodes was studied. By controlling the charging protocol and deposition-dependent material properties, we are able to mitigate self-discharge in these textile-polymer supercapacitors. For the optimized device, more than 90 % of the charge is maintained after five hours, opening the door for practical coupling of these devices into wearable garment devices and self-powered energy harvesting-energy storage circuits.

4. Experimental

4.1. Film deposition

Films of PEDOT-Cl were deposited using a custom-built reactor depicted in Fig. 1 and described in previous reports [32]. Briefly, 3,4-ethylenedioxythiophene (EDOT) (95 %, TCI America), was reacted with iron (III) chloride ($FeCl_3$) (97 %, Sigma Aldrich) in the vapor phase at low pressures maintained at approximately 750 mTorr. EDOT was evaporated at 95 °C and delivered into the chamber via a needle valve (Swagelok SS-4JB) that was typically opened a quarter turn. The volume of EDOT in the glass bulb was carefully monitored over the course of the deposition to ensure an appropriate monomer flow rate of $5-10$ sccm. $FeCl_3$ was sublimed by heating to > 205 °C in a Luxel RADAK II furnace. The substrate stage was heated to 150 °C or 50 °C over the course of the deposition.

Real-time film growth rate was monitored by a quartz crystal microbalance (QCM) located inside the chamber. Due to the different positioning of the QCM relative to the sample stage, a correction factor is needed to account for film growth rate variations. By measuring actual film thickness post-deposition using a Dektak profilometer, a tooling factor of 0.5 was determined. Film growth rate was kept at 2 nm/s. After the desired film thickness was reached, the sample stage was allowed to cool below 60 °C under vacuum. To remove residual iron salts and oligomers, samples were immediately rinsed with dilute acid (0.5 M HCl) for 48 h unless specified, followed by a methanol rinse.

4.2. Device preparation

To create the pseudocapacitive electrodes, carbon cloth swatches (Fuel Cell Earth) were coated with PEDOT-Cl (~1 μm) as described above. Two sections of typically 0.5 × 1 cm were cut and coated with PEDOT-Cl to make up the symmetric electrodes. Two more similarly-sized pieces of cotton cloth were cut and these pieces were then sandwiched between the PEDOT-Cl coated electrodes to fashion the assembled device.

An ambient-stable gel electrolyte was made by mixing 1 g polyvinyl alcohol (PVA) (Mowiol 40–88) with 10 mL DI water, heating the mixture to 90 °C, adding 2.125 g of LiCl as a solid, and stirring the resulting mixture at 90 °C for 2 h before cooling. Once cool, the electrolyte was drop cast onto the assembled device described above, to the extent that all four fabric layers soaked up and became saturated with the electrolyte mixture. This device was then allowed to dry overnight, open to air in a fume hood. The gel electrolyte acted as both an ion conductive material and a crude binder that reliably held the four fabric layers together during the various measurement described in this work.

4.3. Chemical characterization

X-ray diffraction measurements of PEDOT-Cl-coated glass samples were taken using a Smartlab SE II (Rigaku) with a Cu-K-α radiation source.

ICP-MS was taken on PEDOT-Cl-coated carbon cloth samples of varying rinse times. Polymer samples were digested in concentrated nitric acid at 65 °C for several hours before running the measurement.

4.4. Electrochemical characterization

Electrochemical measurements were made using a WaveNow potentiostat from Pine Instruments. Electrical contact to samples and devices was made using platinum foil and Mueller toothless stainless steel (SS) alligator clips to minimize contact resistance and corrosion issues. Stability testing was performed by repeating constant current (2 mA/cm^2) charge-discharge cycles and sampling capacitance values calculated using Eq. (1).

$$C_{device} = i^* \frac{dt}{dV} \tag{1}$$

Specific capacitance values were obtained for PEDOT-Cl coated glass samples which avoids errors associated in determining active mass loading of textile electrodes. For the coated glass samples, active mass

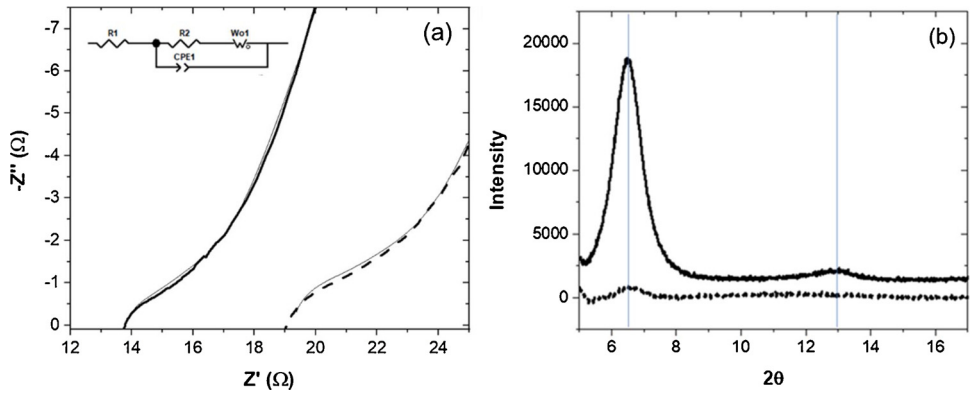

Fig. 6. Characterizations of PEDOT-Cl grown at T_{stage} = 150 °C (solid) and 50 °C (dashed). (a) Impedance spectroscopy of devices with as-deposited electrodes. (b) X-ray diffraction of PEDOT-Cl films on glass.

loading was calculated based on film thickness (~1 μm, measured with a Dektak profilometer), measured area, and a previously reported density of 1.3 g/cm^3 [33]. Three electrode cyclic voltammetry (CV) was performed in 0.5 M aqueous sulfuric acid with a Ag/AgCl reference and a platinum wire counter electrode. Voltage ranged from -0.2 – 0.8 V vs Ag/AgCl. Specific capacitance was calculated using Eq. 2, where A is CV area, v is scan rate, V is voltage window, and m is the active mass.

$$C_{sp} = \frac{A}{v*V*2*m} \tag{2}$$

Doping fraction f of films was calculated as:

$$f = C_{sp}*1V*m*\frac{1}{e}*\frac{1}{NA} \tag{3}$$

Where m is molecular weight of an EDOT monomer, e is elementary charge, and NA is Avogadro's number.

Self-discharge experiments were performed by charging the sample to its final potential at 5 mV/s and subsequently measuring the open circuit potential (OCP) decay. Prior to the OCP step, samples were held at their maximum charging potential (chronoamperometry) for variable amounts of time as a pre-conditioning step. Measurements were taken in a nitrogen filled glovebox as well as in ambient. Voltage rebound experiments were performed by holding at 800 mV for 2 h, discharging to 0 mV at 5 mV/s, holding for 1 min, and then recording the open-circuit voltage recovery.

Electrochemical impedance spectra were taken using an SI 1287 (Solartron Analytical) with an AC amplitude of 2 mV and a frequency range of 300 kHz to 1 Hz. Spectra of three duplicate devices were recorded and the reported charge transfer and Warburg resistances are averages of the set. Presented spectra are representative of the sets (Figure S4).

Conductivity measurements were made using a Signatone four-point probe (S-302-4) with a Keithley 2400 and a DekTak profilometer. Probe spacing was 40mil (~1 mm) and films dimensions were approximately 2 × 2 cm, so a correction factor corresponding to d/s = 20 was used in calculating sheet resistance [34]:

$$Rs = 4.5*\frac{V}{I} \tag{4}$$

where V and I are measured voltage and current. Conductivity was then calculated:

$$\sigma = t/Rs \tag{5}$$

where t is measured thickness and σ is conductivity. Two sets of films were measured, and the conductivity values averaged.

CRediT authorship contribution statement

Wesley Viola: Formal analysis, Investigation, Methodology, Visualization, Writing - original draft. **Chang Jin:** Investigation, Validation, Visualization, Writing - review & editing. **Trisha L. Andrew:** Conceptualization, Funding acquisition, Methodology, Supervision, Writing - review & editing.

Declaration of Competing Interest

The authors declare that they have no known competing financial interests or personal relationships that could have appeared to influence the work reported in this paper.

Acknowledgement

This material is based on work supported by the National Science Foundation under CBET 1706633.

Appendix A. Supplementary data

Supplementary material related to this article can be found, in the online version, at doi:https://doi.org/10.1016/j.synthmet.2020.116483.

References

[1] S.R. Forrest, The path to ubiquitous and low-cost organic electronic appliances on plastic, Nature 428 (2004) 911–918.
[2] L. Zhang, W. Viola, T.L. Andrew, High energy density, super-deformable, garment-integrated microsupercapacitors for powering wearable electronics, ACS Appl. Mater. Interfaces 10 (2018) 36834–36840.
[3] Y.Y. Smolin, K.L. Van Aken, M. Boota, M. Soroush, Y. Gogotsi, K.K. Lau, Engineering ultrathin polyaniline in micro/mesoporous carbon supercapacitor electrodes using oxidative chemical vapor deposition, Adv. Mater. Interfaces 4 (2017) p.1601201.
[4] H.A. Andreas, Self-discharge in electrochemical capacitors: a perspective article, J. Electrochem. Soc. 162 (2015) A5047–A5053.
[5] B.E. Conway, Electrochemical Supercapacitors: Scientific Fundamentals and Technological Applications, Springer Science & Business Media., 2013.
[6] A. Burke, Ultracapacitors: why, how, and where is the technology, J. Power Sources 91 (2000) 37–50.
[7] B.E. Conway, W.G. Pell, T.C. Liu, Diagnostic analyses for mechanisms of self-discharge of electrochemical capacitors and batteries, J. Power Sources 65 (1997) 53–59.
[8] J. Niu, W.G. Pell, B.E. Conway, Requirements for performance characterization of C double-layer supercapacitors: applications to a high specific-area C-cloth material, J. Power Sources 156 (2006) 725–740.
[9] T. Liu, W.G. Pell, B.E. Conway, Self-discharge and potential recovery phenomena at thermally and electrochemically prepared RuO2 supercapacitor electrodes, Electrochim. Acta 42 (1997) 3541–3552.
[10] J.W. Graydon, M. Panjehshahi, D.W. Kirk, Charge redistribution and ionic mobility in the micropores of supercapacitors, J. Power Sources 245 (2014) 822–829.
[11] J. Black, H.A. Andreas, Effects of charge redistribution on self-discharge of electrochemical capacitors, Electrochim. Acta 54 (2009) 3568–3574.
[12] S.E. Rowlands, Electrochemical Supercapacitors for Energy Storage Applications (Doctoral Dissertation, De Montfort University, 2002.
[13] H.A. Andreas, K. Lussier, A.M. Oickle, Effect of Fe-contamination on rate of self-discharge in carbon-based aqueous electrochemical capacitors, J. Power Sources

187 (2009) 275–283.
[14] M.A. Davis, H.A. Andreas, Identification and isolation of carbon oxidation and charge redistribution as self-discharge mechanisms in reduced graphene oxide electrochemical capacitor electrodes, Carbon 139 (2018) 299–308.
[15] H. Olsson, M. Strømme, L. Nyholm, M. Sjödin, Activation barriers provide insight into the mechanism of self-discharge in Polypyrrole, J. Phys. Chem. C 118 (2014) 29643–29649.
[16] L. Zhang, T.L. Andrew, Using the surface features of plant matter to create all-polymer pseudocapacitors with high areal capacitance, ACS Appl. Mater. Interfaces 10 (2018) 38574–38580.
[17] H. Olsson, M. Sjödin, E.J. Berg, M. Strømme, L. Nyholm, Self-discharge reactions in energy storage devices based on polypyrrole-cellulose composite electrodes, Green 4 (2014) 27–39.
[18] K. Shinozaki, A. Kabumoto, H. Sato, K. Watanabe, H. Umemura, S. Tanemura, Mechanism of self-discharge in conductive polymer electrodes, Synth. Met. 38 (1990) 135–141.
[19] F.N. Ajjan, N. Casado, T. Rębiś, A. Elfwing, N. Solin, D. Mecerreyes, O. Inganäs, High performance PEDOT/lignin biopolymer composites for electrochemical supercapacitors, J. Mater. Chem. A 4 (2016) pp.1838-1847.20.
[20] P. Moni, J. Lau, A.C. Mohr, T.C. Lin, S.H. Tolbert, B. Dunn, K.K. Gleason, Growth temperature and electrochemical performance in Vapor-Deposited Poly (3, 4-ethylenedioxythiophene) thin films for high-rate electrochemical energy storage, Acs Appl. Energy Mater. 1 (2018) 7093–7105.
[21] S.E. Atanasov, M.D. Losego, B. Gong, E. Sachet, J.P. Maria, P.S. Williams, G.N. Parsons, Highly conductive and conformal poly (3, 4-ethylenedioxythiophene) (PEDOT) thin films via oxidative molecular layer deposition, Chem. Mater. 26 (2014) 3471–3478.
[22] J.F. Mike, J.L. Lutkenhaus, Electrochemically active polymers for electrochemical energy storage: opportunities and challenges, ACS Macro Lett. 2 (2013) 839–844.
[23] R. Kiebooms, A. Aleshin, K.E.A. Hutchison, F. Wudl, A. Heeger, Doped poly (3, 4-ethylenedioxythiophene) films: thermal, electromagnetical and morphological analysis, Synth. Met. 101 (1999) 436–437.
[24] S. Kaviani, M. Mohammadi Ghaleni, E. Tavakoli, S. Nejati, Electroactive and conformal coatings of oxidative chemical vapor deposition polymers for oxygen electroreduction, ACS Appl. Polymer Mater. 1 (2019) 552–560.
[25] H.A. Andreas, J.M. Black, A.A. Oickle, Self-discharge in manganese oxide electrochemical capacitor electrodes in aqueous electrolytes with comparisons to faradaic and charge redistribution models, Electrochim. Acta 140 (2014) 116–124.
[26] S. Ardizzone, G. Fregonara, S. Trasatti, Inner" and "outer" active surface of RuO2 electrodes, Electrochim. Acta 35 (1990) 263–267.
[27] A.J. Bard, L.R. Faulkner, Fundamentals and applications, Electrochem. Methods 2 (2001) 580–632.
[28] S.P. Arnold, J.K. Harris, B. Neelamraju, M. Rudolph, E.L. Ratcliff, Microstructure-dependent electrochemical properties of chemical-vapor deposited poly (3, 4-ethylenedioxythiophene)(PEDOT) films, Synth. Met. 253 (2019) 26–33.
[29] R.F.L.Q. Giridharagopal, L.Q. Flagg, J.S. Harrison, M.E. Ziffer, J. Onorato, C.K. Luscombe, D.S. Ginger, Electrochemical strain microscopy probes morphology-induced variations in ion uptake and performance in organic electrochemical transistors, Nat. Mater. 16 (7) (2017) 737–742.
[30] K.E. Aasmundtveit, E.J. Samuelsen, O. Inganäs, L.A.A. Pettersson, T. Johansson, S. Ferrer, Structural aspects of electrochemical doping and dedoping of poly (3, 4-ethylenedioxythiophene), Synth. Met. 113 (2000) 93–97.
[31] D.C. Martin, J. Wu, C.M. Shaw, Z. King, S.A. Spanninga, S. Richardson-Burns, J. Hendricks, J. Yang, The morphology of poly (3, 4-ethylenedioxythiophene), Polym. Rev. 50 (2010) 340–384.
[32] D. Bilger, S.Z. Homayounfar, T.L. Andrew, A critical review of reactive vapor deposition for conjugated polymer synthesis, J. Mater. Chem. C 7 (2019) 7159–7174.
[33] X. Wang, X. Zhang, L. Sun, D. Lee, S. Lee, M. Wang, J. Zhao, Y. Shao-Horn, M. Dincă, T. Palacios, K.K. Gleason, High electrical conductivity and carrier mobility in oCVD PEDOT thin films by engineered crystallization and acid treatment, Sci. Adv. 4 (2018) eaat5780.
[34] F.M. Smits, Measurement of sheet resistivities with the four-point probe, Bell Syst. Tech. J. 37 (1958) 711–718.